Harvard-Smithsonian Center for Astrophysics

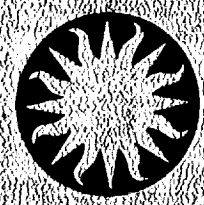

Preprint Series

No. 4900
(Received May 24, 2000)

AN ANALYSIS OF WATER LINE PROFILES IN STAR FORMATION REGIONS OBSERVED BY SWAS

Matthew L.N. Ashby, Edwin A. Bergin, René Plume, John M. Carpenter, David A. Neufeld, Gordon Chin, Neal R. Erickson, Paul F. Goldsmith, Martin Harwit, John E. Howe, Steve C. Kleiner, Dave G. Koch, Brian M. Patten, Rudolf Schieder, Ron L. Snell, John R. Stauffer, Volker Tolls, Zhong Wang, Gisbert Winnewisser, Yun Hei Zhang, and Gary J. Melnick

To appear in
The Astrophysical Journal (Letters)

HARVARD COLLEGE OBSERVATORY
SMITHSONIAN ASTROPHYSICAL OBSERVATORY
60 Garden Street, Cambridge, Massachusetts 02138

Center for Astrophysics
Preprint Series No. 4900

AN ANALYSIS OF WATER LINE PROFILES IN STAR FORMATION REGIONS OBSERVED BY SWAS

Matthew L. N. Ashby, Edwin A. Bergin, René Plume, John M. Carpenter, David A. Neufeld, Gordon Chin, Neal R. Erickson, Paul F. Goldsmith, Martin Harwit, John E. Howe, Steve C. Kleiner, Dave G. Koch, Brian M. Patten, Rudolf Schieder, Ron L. Snell, John R. Stauffer, Volker Tolls, Zhong Wang, Gisbert Winnewisser, Yun Fei Zhang, and Gary J. Melnick

An Analysis of Water Line Profiles in Star Formation Regions Observed by SWAS

M. L. N. Ashby[1], E. A. Bergin[1], R. Plume[1], J. M. Carpenter[2], D. A. Neufeld[3], G. Chin[4], N. R. Erickson[5], P. F. Goldsmith[6], M. Harwit[7], J. E. Howe[5], S. C. Kleiner[1], D. G. Koch[8], B. M. Patten[1], R. Schieder[9], R. L. Snell[5], J. R. Stauffer[1], V. Tolls[1], Z. Wang[1], G. Winnewisser[9], Y. F. Zhang[1], and G. J. Melnick[1]

ABSTRACT

We present spectral line profiles for the 557 GHz $1_{1,0} \rightarrow 1_{0,1}$ ground-state rotational transition of ortho-$H_2^{16}O$ for 18 galactic star formation regions observed by SWAS. Water is unambiguously detected in every source. The line profiles exhibit a wide variety of shapes, including single-peaked spectra and self-reversed profiles. We interpret these profiles using a Monte Carlo code to model the radiative transport. The observed variations in the line profiles can be explained by variations in the relative strengths of the bulk flow and small-scale turbulent motions within the clouds. Bulk flow (infall, outflow) must be present in some cloud cores, and in certain cases this bulk flow dominates the turbulent motions.

Subject headings: ISM:molecules – radio lines:ISM – stars:formation – ISM:clouds

1. Introduction

Water in interstellar space is of great interest for a variety of reasons, among them that it is widely believed to be a significant participant in the chemistry of molecular clouds (Bergin,

[1]Harvard–Smithsonian Center for Astrophysics, 60 Garden St., Cambridge, MA 02138

[2]California Institute of Technology, Dept. of Astronomy, MS 105-24, Pasadena, CA 91125

[3]Dept. of Physics and Astronomy, Johns Hopkins University, 3400 N. Charles Street, Baltimore, MD 21218

[4]NASA Goddard Space Flight Center, Greenbelt, MD 20771

[5]Dept. of Physics and Astronomy, University of Massachusetts, Amherst, MA 01003

[6]National Astronomy and Ionosphere Center, Department of Astronomy, Cornell University, Ithaca NY 14853-6801

[7]511 H Street SW, Washington, DC 20024-2725; also Cornell University.

[8]NASA Ames Research Center, Moffett Field, CA 94035

[9]I. Physikalisches Institut, Universität zu Köln, Zülpicher Strasse 77, D-50937 Köln, Germany

Neufeld, & Melnick 1998) and a major coolant during the later stages of star formation (Ceccarelli, Hollenbach, & Tielens 1996). Unfortunately, most H_2O transitions are obscured by the Earth's atmosphere. Recently the Infrared Space Observatory (ISO) has detected high-energy H_2O transitions towards numerous dense cores (Liseau et al. 1996, Helmich, et al. 1996, van Dishoeck & Helmich, 1996, and Cernicharo et al. 1997), but these transitions tend to be predominantly sensitive to hot gas surrounding young stars (van Dishoeck et al. 1999).

Observations by the recently launched Submillimeter Wave Astronomy Satellite (SWAS) of the 556.936 GHz $1_{1,0} \rightarrow 1_{0,1}$ ground state transition of H_2O have opened another window on water in molecular clouds. This transition, with an upper state energy only 27 K above the ground state, is predicted to be a good probe of the excitation conditions within the extended colder gas surrounding young stars (cf. Liseau & Oloffson 1999). In addition, the high optical depths typically encountered in this line give rise to strong radiative trapping. This combination of traits can lead to significant self-absorption and complex H_2O profiles which contain important information about cloud structure, i.e., the density, temperature, and velocity structure, and even cloud geometry. However, very optically thick lines often fail to exhibit self reversals even in the presence of excitation gradients. This is a problem of long standing in molecular astronomy, which has been addressed by models that vary the relative contributions of local turbulent motions and the bulk velocity field (Goldreich & Kwan 1974, Scoville & Solomon 1974, Martin, Sanders, & Hills 1984, Kwan & Sanders 1986, Juvela 1997). These models reduce the magnitude of self-absorption in the optically thick lines.

In this Letter we present SWAS observations of the 557 GHz $1_{1,0} \rightarrow 1_{0,1}$ transition of ortho-H_2O toward 18 cloud cores. We use spherically symmetric Monte Carlo radiative transfer models to examine the cloud structures that produce these complex spectra.

2. Observations

SWAS has observed numerous dense cores in molecular clouds. The sources presented in this work tend to be massive cloud cores with active star formation and, often, embedded stellar clusters. For a discussion of H_2O emission in less massive cores, see Snell et al. (2000a) and Ashby et al. (2000). SWAS observations of Orion BN/KL are presented in Melnick et al. (2000b), while extended H_2O emission in OMC-1 is discussed in Snell et al. (2000b).

The data were collected in the standard nodding mode (Melnick et al. 2000a) in segments typically 30 minutes long during 1999 January – October. SWAS has a main beam efficiency of 0.9, an average beam width of 3.′8 (FWHM), and a velocity resolution of 0.6 km s^{-1} (Melnick et al. 2000a). Source positions and distances are given in Table 1. Figure 1 presents the SWAS spectra.

3. Results

SWAS has detected H_2O toward every object in Table 1. H_2O emission appears to be ubiquitous in massive cloud cores. The majority of these sources exhibit double-peaked spectra with deep troughs. Most of these troughs coincide closely with the systemic velocity inferred from the simultaneously observed ^{13}CO $J = 5 \rightarrow 4$ line, indicating strong self-absorption in the H_2O line. The others, (e.g., DR 21 and NGC 6334I), are due to absorption by foreground material. Several sources which might superficially appear to be dominated by a single component (e.g., G 265.1+1.5, NGC 2071, and NGC 7538) differ from the 'truly' single-peaked sources in that their H_2O emission peaks are significantly offset from the systemic velocity; we infer they are likewise self-reversed. The spectra presented in this Letter fall roughly evenly into three general categories. Five spectra are single-peaked; six are self-reversed with broad lines (FWHM> 5 km s^{-1}), and seven are self-reversed with relatively narrow lines.

This behavior appears to be reflected by ^{12}CO line profiles in the literature. Sources with self-reversed H_2O lines tend to exhibit self-reversed ^{12}CO $(2 \rightarrow 1)$ profiles. G 265.1+1.5, NGC 2071, and NGC 7538, which superficially appear to be single-peaked, likewise exhibit such reversals (Brand et al. 1984, Phillips et al. 1981, and Kameya et al. 1989). Conversely, our single-peaked sources (G 291.3-0.7, G 322.2+0.6, S 140) are single-peaked in ^{12}CO $(2 \rightarrow 1)$ (Brand et al. 1984, Phillips et al. 1988). M17SW lacks a published ^{12}CO $(2 \rightarrow 1)$ spectrum, but its $3 \rightarrow 2$ and $1 \rightarrow 0$ spectra are both single-peaked (Martin, Sanders, & Hills 1984). Thus it appears that the physical conditions affecting the ^{12}CO line influence the H_2O line in an analogous manner. This is somewhat surprising since ^{12}CO and H_2O have such different critical densities.

Significant broad (10-15 km s^{-1}) H_2O emission is detected in most sources, centered on the systemic cloud velocities. These broad wing features are presumably from H_2O entrained in known high-velocity outflows present in the $3'.3 \times 4'.5$ SWAS beam, e.g., ρ Oph A, Ceph A, DR 21, NGC 1333, NGC 2071, NGC 6334I, NGC 7538, and S 140. See Neufeld et al. (2000) for a discussion of SWAS spectra of molecular outflows.

4. Monte Carlo Models of H_2O Emission

The variety of H_2O line profiles shown in Figure 1 suggests that there are differing physical conditions within their clouds of origin. Since many of the clouds have quite similar density (Snell et al. 1984, Mundy et al. 1986, Bergin, Snell, & Goldsmith 1996, and Snell et al. 2000a), and temperature (Bergin et al. 1994, Churchwell & Hollis 1983) structures, velocity structure likely plays an important role in line formation (cf. Kwan & Sanders 1986).

To test this idea we have developed a Monte Carlo radiative transfer code to examine how physical structure affects line formation for the 557 GHz transition. The Monte Carlo treatment provides a careful global accounting of photon absorption and reemission that is missing

from simpler (but computationally faster) models such as the Large Velocity Gradient (LVG) approximation. Our code is a modified version of the original Bernes (1979) code, to which we added a treatment of continuum photons from dust mixed with the gas. Our code has been extensively tested by comparing its results to those obtained using escape probability methods in the LVG limit and to those generated by the Accelerated Lambda Iteration (ALI) code of J. Zmuidzinas in the static limit. The code uses a physical model consisting of a spherically symmetric cloud subdivided into an arbitrary number of shells. Physical conditions may vary within a cloud but are held constant within each shell. The ability to vary physical parameters arbitrarily affords great flexibility.

This code allows us to determine how different contributions from turbulent and outflow motions affect the simulated line profile. Our approach was to construct a family of simple constant temperature and density models ($T = 30$ K, $n_{\rm H_2} = 10^5$ cm^{-3}) of spherical outflow and infall. For the outflow models (Figure 2), the velocity, v, is zero at the cloud center and increases linearly to v_{RMAX} at the cloud edge. To create infall models (Figure 3) we subtracted v_{RMAX} from the outflow model velocity fields, which yields a velocity equal to zero at the cloud edge and decreasing toward the cloud center. We varied the relative strengths of the local turbulent velocity width v_{TURB} and the bulk velocity field while holding the sum of the two contributions constant, i.e., $V_0 = (v_{TURB}^2 + (2v_{RMAX})^2)^{1/2}$ for outflow and $V_0 = (v_{TURB}^2 + (2v_{CEN})^2)^{1/2}$ for infall, where v_{CEN} is the velocity at the cloud center. We chose a total width of $V_0 = 4.0$ km s^{-1}, and set $RMAX = 0.2$ pc, these values being typical for the sources in Figure 1. We assume a power law of the form $\kappa = \kappa_0(\lambda/\lambda_0)^{-1.5}$ cm^{2}g^{-1} for the opacity per gram of dust and gas, where $\lambda_0 = 1300$ μm and $\kappa_0 = 5 \times 10^{-3}$ cm^2 g^{-1} (Goldsmith et al. 1997, Hildebrand 1983). Within each shell we interpolate Phillips et al. (1996) collision rates for ortho- and para-H_2 to derive rates appropriate for the given temperature of 30 K. We assume a ratio of ortho- to para-H_2 of 0.1, and a volume filling factor of unity. We modeled five energy levels in the ortho-H_2O molecule, i.e., all levels up to T$\sim$ 200 K.

Though these models are simplistic compared to more physical treatments (e.g., Shu (1977) infall), they are nonetheless effective in illustrating the effects of bulk flow on the H_2O spectra. The model spectra exhibit single-peaked lines when bulk flows dominate. Self-absorption results when turbulent motions dominate. When both components of the velocity field are comparable, an obvious asymmetry is apparent. For the model spectra in Figure 2, the blue peak is weaker, as expected, for outflow models. The opposite asymmetry occurs for the infall models. Though bulk flows appear to dominate in most cases, the model spectra presented here exhibit the full range of profiles seen in the SWAS data. For example, NGC 2024 has a spectrum that may be compared to the $v_{TURB}/2v_{RMAX} = 0.75$ model, i.e., a model in which both contributions to the velocity field are comparable. On the other hand, any of the models in which bulk flow is dominant appears to agree better with the 557 GHz H_2O spectrum of M17SW. Finally, infall models with a small contribution from turbulent motions resemble the spectra of G267.9-1.1 and NGC 6334I. Detailed models of S 140 and ρ Oph A are discussed in Ashby et al. (2000).

5. Summary

The SWAS spectra presented here demonstrate that 557 GHz H_2O emission is common in massive cloud cores. The line profiles vary greatly from source to source, but a common feature is a broad component attributable to known outflows within the SWAS beam. In addition, the spectra are typically either single-peaked, self-absorbed with broad components, or self-absorbed with relatively narrow components. CO line profiles may be useful as predictors of the ortho-H_2O line profiles. The profiles' variety can be attributed to differences in the relative contributions of the bulk flow and the turbulent motions to the overall velocity field; bulk flows may in some cases dominate the turbulent motions for the 557 GHz water line.

The authors gratefully acknowledge helpful discussions with P. Myers and M. Crosas. J. Zmuidzinas generously made his ALI code available. This work was supported by NASA Grants NAS5-30702, NAG5-3542, and NASA's Long Term Space Astrophysics Program.

REFERENCES

Ashby, M. L. N., et al. 2000, ApJ, this volume

Bergin, E. A., Goldsmith, P. F., Snell, R. L., and Ungerechts, H. 1994, ApJ, 431, 674

Bergin, E. A., Snell, R. L., and Goldsmith, P. F. 1996, ApJ, 460, 343

Bergin, E. A., Neufeld, D. A., and Melnick, G. J. 1998, ApJ, 499, 777

Bernes, C. 1979, A&A, 73, 67

Brand, J., van der Bij, M. D. P., de Vries, C. P., Israel, F. P., de Graauw, T., van de Stadt, H., Wouterloot, J. G. A., Leene, A., and Habing, H. J. 1984, A&A, 139, 181

Ceccarelli, C., Hollenbach, D. J., and Tielens, A. G. G. M. 1996, ApJ, 471, 400

Cernicharo, J., Lim, T., Cox, P., Gonzalez-Alfonso, E., Caux, E., Swinyard, B. M., Martin-Pintado, J., Baluteau, J. P., and Clegg, P. 1997, A&A, 323, L25

Churchwell, E., and Hollis, J. M. 1983, ApJ, 272, 591

Goldreich, P., and Kwan, J. 1974, ApJ, 189, 441

Goldsmith, P. F., Bergin, E. A., and Lis, D. 1997, ApJ, 491, 615

Helmich, F.P., et al. 1996, A&A, 315, L173

Hildebrand, R. H. 1983, QJRAS, 24, 267

Juvela, M. 1997, A&A, 322, 943

Kameya, O., Hasegawa, T. I., Hirano, N., Takakubo, K., and Seki, M. 1989, ApJ, 339, 222

Kwan, J., and Sanders, D. B. 1986, ApJ, 309, 783

Liseau, R., et al. 1996, A&A, 315, L181

Liseau, R., and Olofsson, G. 1999, A&A, 343, L83

Martin, H. M., Sanders, D. B., and Hills, R. 1984, MNRAS, 208, 35

Melnick, G., et al. 2000a, ApJ, this volume

Melnick, G., et al. 2000b, ApJ, this volume

Mundy, L. G., Scoville, N. Z., Bååth, L. B., Masson, C. R., and Woody, D. P. 1986, ApJ, 304, L51

Neufeld, D.A., et al. 2000, ApJ, this volume

Phillips, J. P., White, G. J., Rainey, R., Avery, L. W., Richardson, K. J., Griffin, M. J., Cronin, N. J., Monteiro, T., and Hilton, J. 1988, A&A, 190, 289.

Phillips, T. G., Knapp, G. R., Hubbins, P. J., Werner, M. W., Wannier, P. G., Neugebauer, G., and Ennis, D. 1981, ApJ, 245, 512

Phillips, T. R., Maluendes, S., and Green, S. 1996, ApJS, 107, 467

Scoville, N. Z., and Solomon, P. M. 1974, ApJ, 187, L67

Shu, F. H. 1977, ApJ, 214, 488.

Snell, R. L., Mundy, L. G., Goldsmith, P. F., Evans, N. J., and Erickson, N. R. 1984, ApJ, 276, 625

Snell, R. L., et al. 2000a, ApJ, this volume

Snell, R. L., et al. 2000b, ApJ, this volume

van Dishoeck, E., and Helmich, F. P. 1996, A&A, 315, L177

van Dishoeck, E., et al. 1999, in *The Universe as Seen by ISO*, eds. Cox, P., Demuyt, V., and Kessler, M. ESA Special Publications Series (SP-427)

This preprint was prepared with the AAS LaTeX macros v4.0.

Table 1. Targets Observed by SWAS

SOURCE	POSITION (J2000) α	δ	DISTANCE (pc)
W3-OH	2:27:02.8	61:52:21	2200
N1333-IRAS4	3:29:10.5	31:13:35	350
OMC-1(0,-3.2)	5:35:14.5	-5:25:49	415
NGC 2024	5:41:44.5	-1:55:35	415
NGC 2071	5:47:04.1	0:21:43	390
NGC 2264SC-N	6:41:03.9	9:34:39	800
G267.9-1.1	8:59:12.0	-47:29:04	1700
G265.1+1.5	8:59:23.3	-43:46:14	1000
G268.4-0.9	9:01:54.3	-47:43:59	800
G291.3-0.7	11:11:37.7	-61:19:49	2400
G322.2+0.6	15:18:35.2	-56:38:25	3800
ρ OPH A	16:26:23.4	-24:23:02	160
NGC 6334I	17:20:53.0	-35:44:57	1740
M17SW	18:20:22.1	-16:12:37	2200
DR 21	20:39:00.9	42:19:38	3000
S140	22:19:17.1	63:18:46	910
CEPH A	22:56:17.9	62:01:50	730
NGC 7538	23:13:47.6	61:26:54	2800

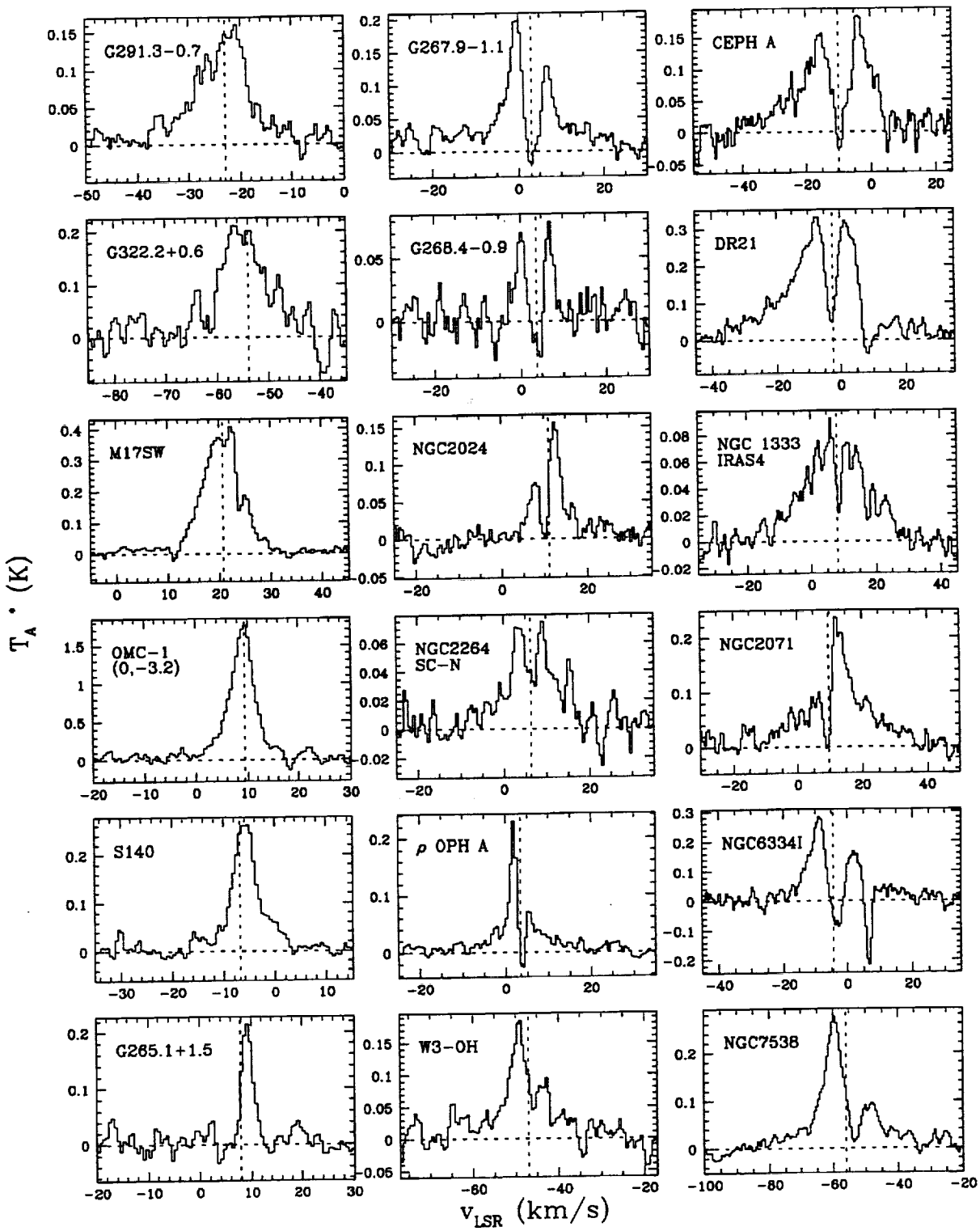

Fig. 1.— SWAS spectra of the 557 GHz transition of ortho-H_2O. Dotted vertical lines mark the fitted line center velocity of the simultaneously observed 550.926 GHz ^{13}CO $J = 5 \rightarrow 4$ transition. OMC-1(0,-3.2) was observed at α =5:35:14.5, δ =-5:25:49 (J2000), 3′.2 south of the BN/KL object. A first-order baseline has been subtracted from the data. Double-peaked spectra have been placed in the right-hand (relatively broad lines) and center (relatively narrow lines) columns, and the left-hand column contains single-peaked spectra (but see the discussion of G265.1+1.5 in the text).

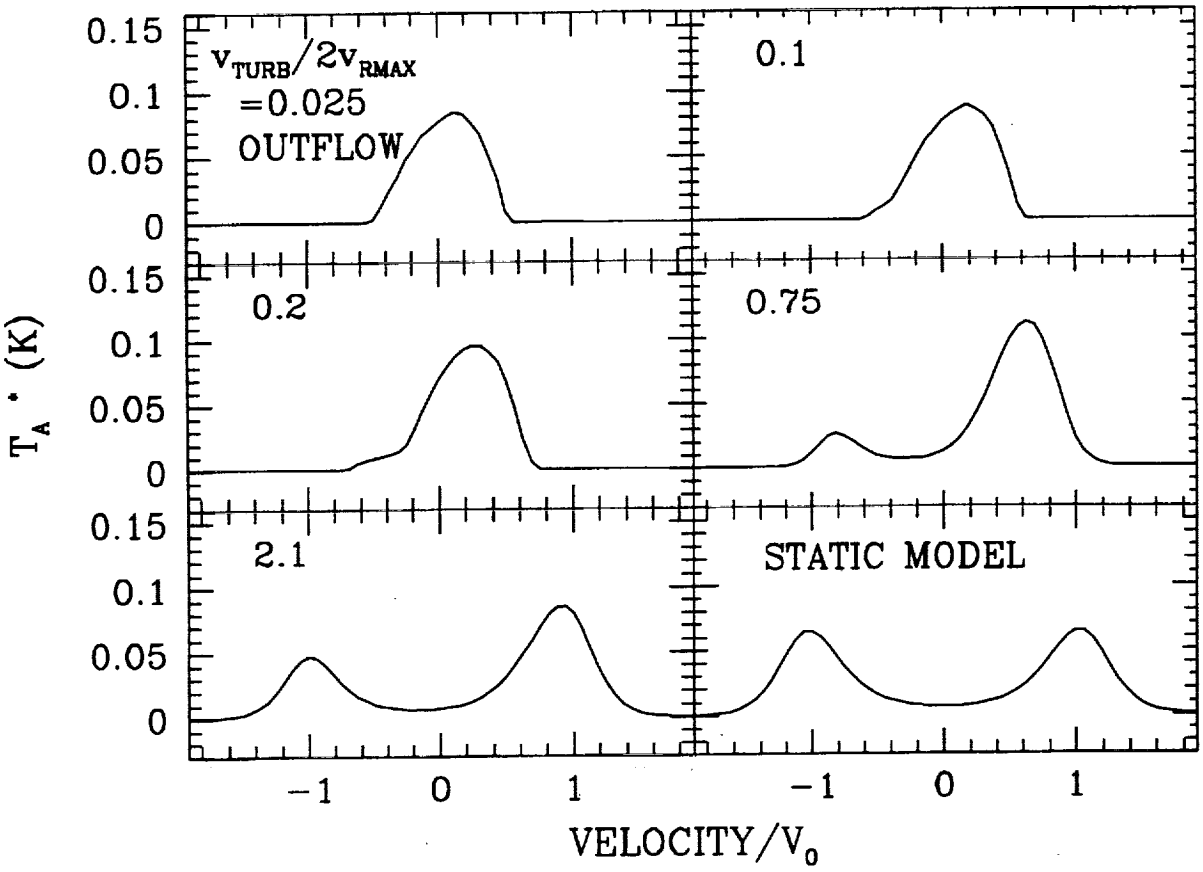

Fig. 2.— Monte Carlo model 557 GHz H_2O spectra for spherical outflow in clouds with constant temperature and density, in which the relative contributions of the turbulent velocity and the linear spherical outflow velocity field to the total velocity V_0 are varied as described in the text.

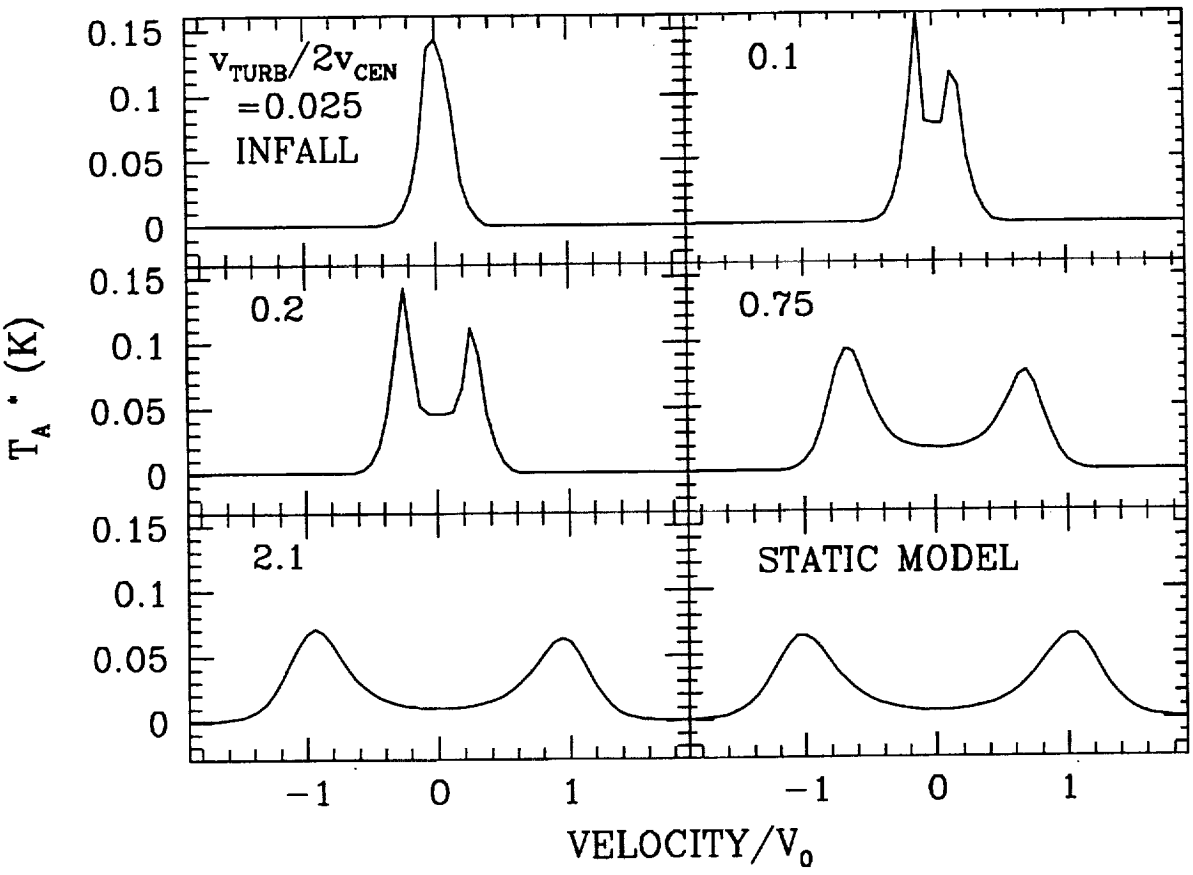

Fig. 3.— As Figure 2, but for clouds undergoing spherical infall.